Landscape Ecology **13:** 167–186, 1998.

The behavior of landscape metrics commonly used in the study of habitat fragmentation

Christina D. Hargis[1,*], John A. Bissonette[1] and John L. David[2]
[1]*Utah Cooperative Fish and Wildlife Research Unit, U.S. Geological Survey Biological Resources Division, College of Natural Resources, Utah State University, Logan, UT 84322–5290, USA;* [2]*Foundation for Ecological Restoration, Monitoring, and Assessment, 3213 Montreal N.E., Albuquerque, NM 87111, USA;* [*]*Current address: Rocky Mountain Forest and Range Experiment Station, Southwest Forest Science Complex, 2500 S. Pine Knoll, Flagstaff, AZ 86001–6381*

Received 18 July 1996; Revised 3 May 1997; Accepted 15 July 1997

Keywords: landscape ecology, landscape measures, fragmentation, mean proximity index, perimeter-area fractal dimension, mass fractal dimension

Abstract

A meaningful interpretation of landscape metrics is possible only when the limitations of each measure are fully understood, the range of attainable values is known, and the user is aware of potential shifts in the range of values due to characteristics of landscape patches. To examine the behavior of landscape metrics, we generated artificial landscapes that mimicked fragmentation processes while controlling the size and shape of patches in the landscape and the mode of disturbance growth. We developed nine series of increasingly fragmented landscapes and used these to investigate the behavior of edge density, contagion, mean nearest neighbor distance, mean proximity index, perimeter-area fractal dimension, and mass fractal dimension. We found that most of the measures were highly correlated, especially contagion and edge density, which had a near-perfect inverse correspondence. Many of the measures were linearly-associated with increasing disturbance until the proportion of disturbance on the landscape was approximately 0.40, with non-linear associations at higher proportions. None of the measures was able to differentiate between landscape patterns characterized by dispersed versus aggregated patches. The highest attainable value of each measure was altered by either patch size or shape, and in some cases, by both attributes. We summarize our findings by discussing the utility of each metric.

Introduction

Investigations of ecological phenomena at broad spatial scales often require quantifiable descriptions of landscape pattern and structure for testing relationships or making predictions about the landscape and the phenomena in question. To this end, a variety of landscape metrics have been developed (Forman and Godron 1986; O'Neill et al. 1988; Turner 1990; Milne 1991; Musick and Grover 1991; Gustafson and Parker 1992; Li and Reynolds 1993, McGarigal and Marks 1995).

A meaningful interpretation of landscape metrics is possible only when the limitations of each measure are fully understood, the range of attainable values is known, and the user is aware of potential shifts in the range of values when applied to landscapes with different structural characteristics. A mathematical analysis of expected values can be done using the equations for each spatial measure. However, ecologists with less exposure to mathematical theory will frequently gain more appreciation of spatial measures by an empirical approach. Gustafson and Parker (1992) provided an important step in understanding spatial metrics by using simulated landscapes to explore the relationship between the proportion of forest cover and several indices of spatial pattern. They generated two kinds of landscapes: one using randomly placed pixels, and the other using randomly-placed rectilinear patches. For each landscape metric, the

response functions derived from random pixel maps and random clump maps were graphically compared.

Our study was motivated by an interest in applying spatial measures to actual landscapes of fragmented forest cover that differed substantially in appearance from the random clump maps generated by Gustafson and Parker (1992), due to larger patches, smoother perimeters, and greater interpatch distances than those produced by random clump simulations. Our underlying question was whether differences between random clump maps and actual landscapes, in terms of patch size, shape, or placement, would significantly alter the response functions of spatial metrics. To test this, we developed a computer program under the name Landscape Simulator for Fragmentation (LSF) that allowed us to simulate a wide variety of landscapes while systematically controlling the size, shape, and placement of patches. We then replicated the procedures and methodology of Gustafson and Parker (1992), using many of the same landscape metrics and adding other measures that commonly are applied to studies of habitat fragmentation.

For each landscape metric examined, we asked the following questions:

1. Does the metric provide unique information, as evidenced by low correlation with other landscape measures?
2. Does the size or shape of landscape patches alter the possible range of values of the metric?
3. Does the mode of disturbance growth alter the possible range of values of the metric?
4. Is the metric sensitive to the spatial distribution of patches?

Methods

Generating landscapes

The LSF program was designed to imitate raster-based GIS maps of any user-defined size. Our maps were 101 by 101 pixels in extent, which approximated a 918 ha map extent when 30-m pixel resolution was assumed. This extent and grain size mimicked LANDSAT Thematic Mapper images for study areas the size of individual watersheds, timber sales, and fire events. Artificial landscapes with 101^2 pixels were used for the majority of our investigations, but we also built series of landscapes having 64^2, 128^2, 256^2, and 512^2 pixels to test the effects of map extent on the behavior of the measures.

We began with a map filled by a single cover type *i*, which formed the map matrix and represented the original cover type, and disturbed the continuity of this matrix with cover type *j*. We randomly selected patches of type *j* from a data base and placed each patch at a random point on the map until a desired proportion of disturbance was reached. Each successive landscape represented an incremental increase in the proportion of disturbance (P_j) from 0.05–0.95 of the map, at 0.10 proportional intervals. The actual P_j for each landscape was constrained to fall no more than 0.006 below the specified value.

Disturbance patches used for building fragmented landscapes conformed to one of three possible patch types, with each landscape built from only one type. The first type consisted of small rectangles similar to the random clump maps developed by Gustafson and Parker (1992). The data base consisted of 75 rectangular patches ranging in size from 1–25 pixels with edge lengths of 1–5 pixels (Fig. 1).

The second patch type was characterized by small, irregular-shapes with the same patch size frequency distribution as the data base of rectangular patches (Fig. 2). The mean patch size of both rectangular and small-irregular patches was 9 ± 6.4 pixels.

The third patch type was created to simulate habitat fragmentation resulting from the clearcut method of timber harvest commonly used in managed forest ecosystems (Fig. 3). To generate realistic clearcut landscapes, we created a data base of 109 actual timber clearcut harvest patches from the Uinta Mountains of northern Utah. Clearcut patch size ranged from 0.6–36 ha (7–400 pixels) with a mean of 10 ± 6.9 ha (115 ± 76.3 pixels), and the patch size frequency distribution was controlled to be the same as that derived from a subset of 18, 9 km^2 landscape windows in the Uinta Mountains.

Clearcut patches from the Uinta Mountains were typical of harvest blocks located on National Forest System lands in western states. On federal lands, the current upper limit of clearcut harvest blocks for most forest types is 16 ha, as set by 36 CFR Part 219 (Department of Agriculture 1982) under the National Forest Management Act of 1976. Clearcuts greater than 16 ha occasionally are approved at the regional level of the Forest Service if adequate justification is provided. Economic considerations, as well as the difficulty in accurately mapping small tracts of land, typically creates a lower size limit of 2 ha, although exceptions below this size occur. The shapes of clearcut patches are often irregular, either from the standpoint

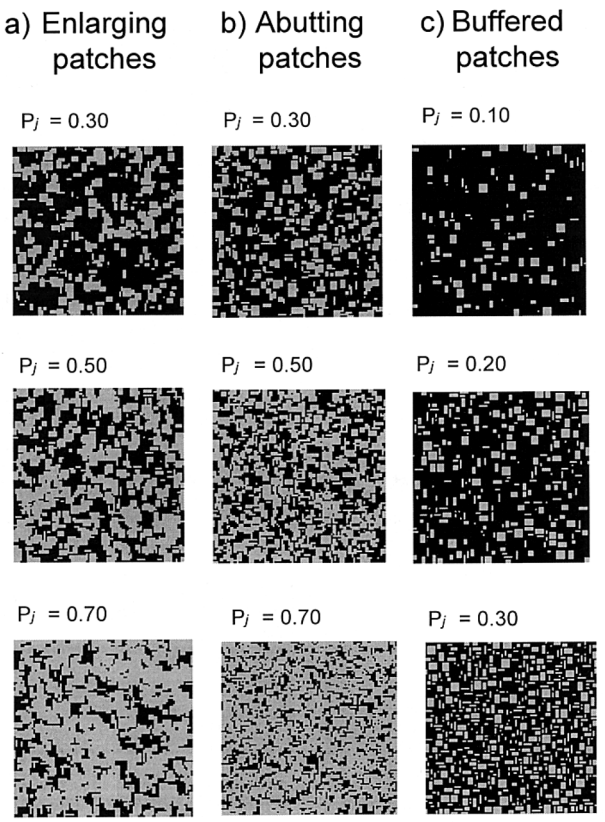

Figure 1. Simulated landscapes built from rectangular patches using three modes of disturbance growth, with black representing original habitat and gray representing disturbance. Enlarging and abutting patch landscapes are shown at representative disturbance levels of 0.30, 0.50, and 0.70, whereas buffered patch landscapes are shown at 0.10, 0.20, and 0.30 levels of disturbance, because the buffered patch series did not exceed 0.40.

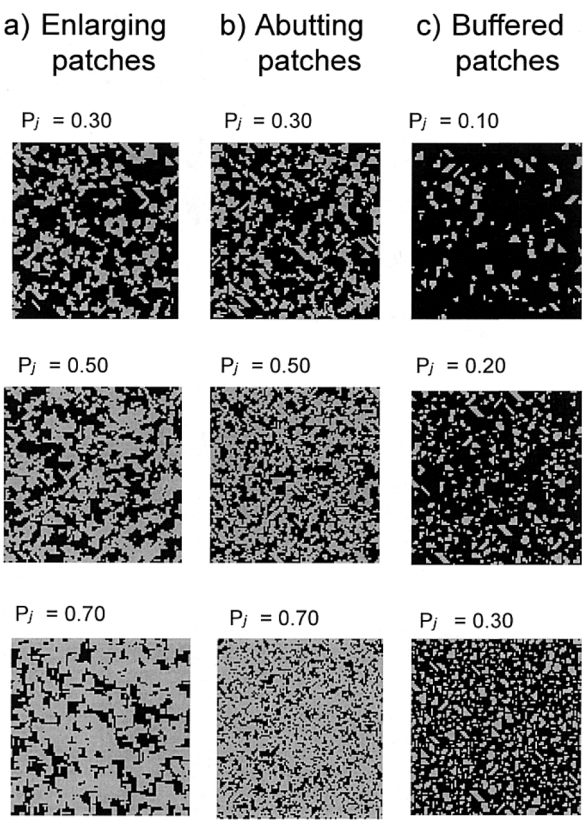

Figure 2. Simulated landscapes built from small, irregular patches using three modes of disturbance growth, with black representing original habitat and gray representing disturbance. Enlarging and abutting patch landscapes are shown at representative disturbance levels of 0.30, 0.50, and 0.70, whereas buffered patch landscapes are shown at 0.10, 0.20, and 0.30 levels of disturbance, because the buffered patch series did not exceed 0.40.

of landscape design for scenic values, or due to topographic constraints.

With all three data bases, the patches were internally contiguous; that is, they did not contain internal holes unoccupied by cover type *j*. We used only one patch type in the construction of any given landscape.

In addition to modeling three types of patch configuration, we modeled three types of disturbance growth: enlarging patches, abutting patches, and buffered patches. Landscapes built from enlarging patches approximated the growth of disturbances that spread from nuclei, such as fire and insect infestations. Landscapes built from buffered patches simulated discrete disturbance events, such as the clearcut method of timber harvest, in which each additional harvest patch is a discrete unit separated from other harvest patches by forest buffers. Landscapes built from abutting patches represented an intermediary stage between enlarging and buffered patch disturbance growth.

Disturbance growth patterns were generated by establishing rules in which patches were placed on a landscape. To simulate patch enlargement, we allowed patches to overlap as they were placed on the map (Figs. 1a, 2a, 3a). For abutting patches, the added patches could share boundaries with existing patches, but overlap was not allowed (Figs. 1b, 2b, 3b). To mimic the growth of disturbance from buffered patches, each successive patch was placed a minimum of two pixels from existing patches (Figs. 1c, 2c, 3c).

We built nine landscape series of increasing disturbance, using one patch type and disturbance growth pattern per series. Each series consisted of five landscape simulations per proportional interval of distur-

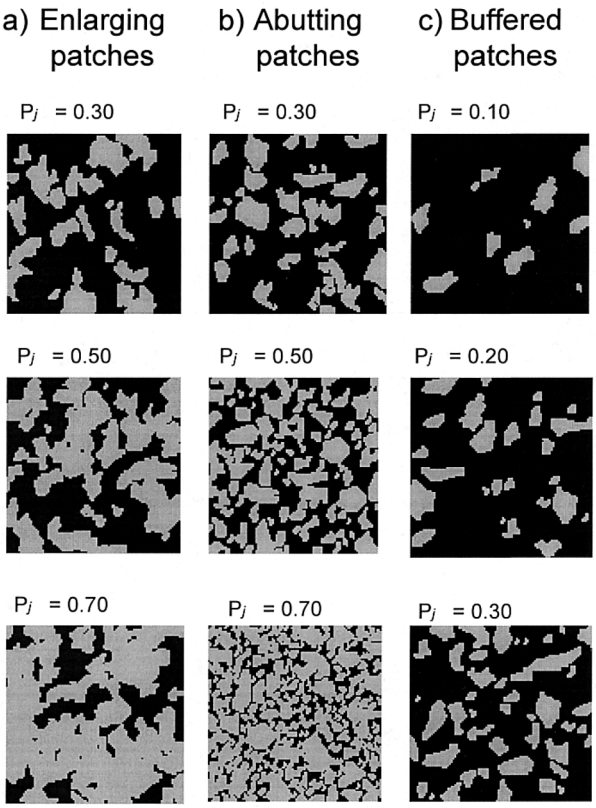

Figure 3. Simulated landscapes built from clearcut patches using three modes of disturbance growth, with black representing original habitat and gray representing disturbance. Enlarging and abutting patch landscapes are shown at representative disturbance levels of 0.30, 0.50, and 0.70, whereas buffered patch landscapes are shown at 0.10, 0.20, and 0.30 levels of disturbance, because the buffered patch series did not exceed 0.40.

bance. Sample sizes of each landscape series ranged from 30–50 depending on the patch type and disturbance growth pattern used. Due to constraints imposed by the abutting and buffered patch rules, not all landscapes reached disturbance levels of 0.95. For clearcut patch landscapes built with the abutting patch rule, the landscape series was truncated at a maximum patch density of 0.70 because clearcut patches were too large to fit in the remaining matrix unless patch overlap was allowed. The buffered patch rule constrained the maximum disturbance attainable for all patch types, because irregular patch shapes left isolates of original habitat too small for additional patches. Moreover, buffers between patches occupied more than half of each landscape. P_j did not exceed 0.40 for landscapes built with clearcut patches, and was limited to 0.35 for rectangular patch maps and 0.30 for small-

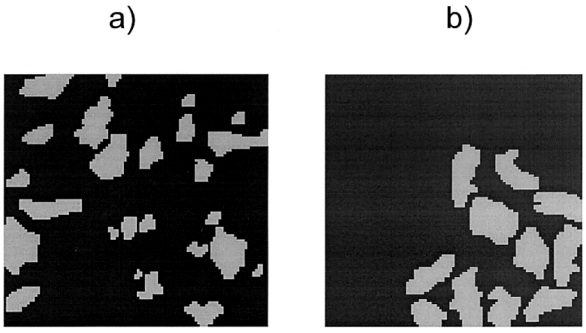

Figure 4. Simulated landscapes at P_j = 0.20, with patches a) dispersed and b) aggregated.

irregular patch maps. Because of the narrower range of P_j for landscapes made from buffered patches, we increased disturbance at increments of 0.05 rather than 0.10 while maintaining five landscapes per increment.

The buffered-patch rule altered the patch size distribution when the proportion of disturbance was high. As landscapes approached the maximum P_j, smaller patches were used to fill the remaining space, and the average patch size of the resulting landscapes was smaller than that of other landscapes.

Random placement of patches on landscapes generally resulted in dispersed patterns that were not useful for determining whether fragmentation measures could differentiate aggregated versus dispersed spatial distributions of patches. To test for pattern sensitivity, we created an additional landscape series of clearcut patches in which we forced patches to be aggregated by using the discrete patch placement rule and specifying that all patches be no further than three pixels apart (Fig. 4). We then compared the aggregated patterns with the original, dispersed clearcut patterns.

LSF was written in the Khoros® image processing environment on Sun Sparc stations. Simulations were run on an IBM RS6000/370 network at the Albuquerque Resource Center, University of New Mexico.

Measuring fragmentation

Landscape measures selected for analysis were edge density, contagion, mean nearest neighbor distance, proximity index, perimeter-area fractal dimension, and mass fractal dimension, which are defined below. We used the FRAGSTATS spatial pattern analysis program ver. 2.0 (McGarigal and Marks 1995) to calculate the first five measures listed. Algorithms used in these calculations are listed in Appendix C of the

FRAGSTATS manual (McGarigal and Marks 1995). The mass fractal dimension was calculated using software developed by B. Milne and T. Keitt at the University of New Mexico under NSF grant BSR–9107339 and included as an add-on toolbox within the Khoros image processing environment.

Edge density is the total length of patch edge per unit area within each landscape (McGarigal and Marks 1995), which we expressed as km of edge per ha**.** This measure is sensitive to map resolution, since fine resolution yields greater edge length, and is therefore useful only for comparison between landscapes with a common grain size. We calculated edge density using pixels connected both side to side and diagonally.

Contagion describes the extent to which pixels are aggregated, and is calculated in FRAGSTATS as the sum of two probabilities: the probability that a pixel belongs to cover type *i*, equivalent to the proportional representation of the cover type on the map, and the conditional probability that, given a pixel is type *i*, that one of the neighboring cells is cover type *j* (McGarigal and Marks 1995). The FRAGSTATS contagion index was calculated from an algorithm developed by Li and Reynolds (1993), a modification of the original form presented by O'Neill et al. (1988).

The proximity index (Whitcomb et al. 1981, Gustafson and Parker 1992) measures the isolation of a patch within a complex of patches, given a specified search radius. It is calculated as the sum, for all patches within the search radius, of the ratio of patch size to nearest neighbor edge-to-edge distance. The mean proximity index for a landscape is the average proximity index derived from all patches. Comparisons between maps are only possible if the search radius is the same for all maps. We used a search radius of 10 pixels to allow comparison of our results with those of Gustafson and Parker (1992). However, FRAGSTATS (McGarigal and Marks (1995) calculated the distances from a focal patch to each patch within the search radius, whereas Gustafson and Parker (1992) calculated the nearest neighbor distance of all patches within the search radius. Using FRAGSTATS, we were unable to standardize the proximity index in the manner described by Gustafson and Parker (1992), and instead conducted our analysis on the absolute values of the proximity index. Patch areas were calculated using connections of pixels on the four adjacent sides and diagonals.

Mean nearest neighbor distance defines the average edge-to-edge distance (m) between a patch and its nearest neighbor in the landscape. It differs from the mean proximity index in that patch area is not used in the calculation, and distances are between nearest patches rather than between all patches within a search radius. This index yields absolute values and requires maps of similar extent and known grain size for comparisons.

Perimeter-area fractal dimension provides information on the irregularity of patch edge. Perimeter-area fractal dimension was computed by FRAGSTATS as 2 divided by the slope of log(P) on log(A), where P and A are the perimeter (m) and area (m^2) of each patch (McGarigal and Marks 1995), and an average value was computed for all patches on a landscape. The theoretical limits of this measure are between one and two, with higher values indicating greater complexity of patch edge (Lovejoy 1982). The term "perimeter" in McGarigal and Marks (1995) is used to describe the outermost occupied pixels of a patch, whereas in the physics literature, these pixels are known as a special form of edge called the "hull", and the term "perimeter" is reserved for the unoccupied pixels adjacent to the hull (Voss 1984, Grossman and Aharony 1987). We will retain the term perimeter-area fractal dimension in reference to the measure calculated by FRAGSTATS, but will refer to the outermost occupied pixels of a patch as the edge rather than the perimeter.

Mass fractal dimension quantifies total complexity of the map matrix rather than irregularity of individual patches. This measure describes the scaling relationship between the number of pixels of a given cover type within a sample of the landscape, and the size of the box defining the sample. Box sizes range from a minimum of 3–5 pixels on a side, to a maximum of approximately 1/3 of the landscape. We calculated mass fractal dimension for cover type *i* using sampling boxes with edge lengths of 3, 9, 15, 21, and 27 pixels. We counted all pixels of cover type *i* within the box when it was centered on each *i* pixel on the map, and derived a mean value of total *i* pixels per box size. Mass fractal dimension was the slope derived from regressing the log of the mean number of pixels in each size of box on the log of the box lengths (Voss 1988, Milne 1991). The theoretical limits of this measure lie between zero and two. A value of two is achieved when the cover type of interest completely fills the 2-dimensional map or occurs in a regular pattern that covers the entire map, and lower values are derived when either of these conditions are altered by the presence of a second cover type.

Analyzing the behavior of fragmentation measures

We analyzed the behavior of each fragmentation measure over the full range of disturbance by regressing each measure against increasing P_j within each landscape series. We examined the effects of patch size and patch shape by using multiple regression techniques to compare fragmentation values generated by rectangular, small-irregular, and clearcut patch configurations. Where significant differences in the values of a fragmentation measure occurred among patch configurations, we conducted pair-wise comparisons of regression coefficients using a Fisher's LSD (Kleinbaum et al. 1988) to determine the source of the difference.

We added a quadratic term to the regression models for the analysis of contagion, total edge, mass fractal dimension and perimeter-area fractal dimension, to make a better fit of the data to the regression line. For nearest neighbor distance, a log-log transformation was applied to account for non-linearity in the response curves. We were unable to conduct a regression analysis on mean proximity index because of the high variance in observed values at high values of P_j, and chose to analyze this variable qualitatively.

We compared the effects of each type of disturbance growth qualitatively rather than through a regression analysis, because landscape series using abutting and discrete patches did not cover the full range of P_j. This was done through a visual comparison of the fragmentation measures' response curves generated for landscapes under each of the patch placement rules.

Results

Correlations between landscape metrics

We examined correlations between P_j and each of the landscape metrics, as well as between all possible pairs of metrics. We were interested in the strength of the correlation, rather than the direction, and therefore italicized all $|r| > 0.80$ (Tables 1, 2, and 3). Across all comparisons, the range of correlation coefficients was fairly similar regardless of whether the landscapes contained small rectangular patches (Table 1), small irregular patches (Table 2) or clearcut patches (Table 3). However, the type of disturbance growth affected the strength of the relationship. Generally speaking, correlations were highest when disturbance growth was with buffered patches (Tables 1, 2, and 3), partly due to the quasi-linear response asssociated with landscapes limited to the 0.05–0.35 range of disturbance proportions.

The $|r|$ between P_j and each landscape metric (first row of each subtable in Tables 1, 2, and 3) ranged from 0.12–0.99, and 43% of these relationships had $|r| > 0.80$ (Tables 1, 2, and 3). Correlations were highest when disturbance growth was with abutting and buffered patches. This was particularly true for edge density, contagion, and mass fractal dimension, implying that relative changes in these measures could be approximated simply by examining changes in the proportion of disturbance on a landscape.

Among metrics, correlations were highest between all paired combinations of edge density, contagion, and mass fractal dimension. For landscapes with small patches, correlations were also high between these three measures and mean proximity index (Tables 1 and 2). On landscapes where patch size was small and also buffered, these measures were nearly perfectly correlated. Graphed representations of edge density and contagion over increasing disturbance were almost mirror images (Figs. 5 and 6).

Effects of patch size

We found significant differences ($P < 0.001$) in the expected values of all fragmentation measures due to the size of patches involved in the fragmentation process (Tables 4, 5, and 6). Landscapes with clearcut patches had consistently lower values of edge density (Fig. 5) and higher values of contagion (Fig. 6) than either of the smaller patch landscapes. Mean nearest neighbor distance appeared to be sensitive to patch size only when patches were sparsely distributed on the landscape (low P_j) (Fig. 7), resulting in more variation in inter-patch distance for large-patch landscapes. Landscapes containing few, large clearcuts had higher mean distances between patches than landscapes containing many, small clearcuts.

The proximity index also was sensitive to patch size, with large patch landscapes having lower values and greater variance than small patch landscapes when disturbance growth was with enlarging or abutting patches (Fig. 8a and b). This relationship was reversed under the buffered patch rule, and large patch landscapes had higher values (Fig. 8c).

Perimeter-area fractal dimension appeared sensitive to patch size when disturbance was with enlarging or abutting patches, with lower values derived from large-patch landscapes (Fig. 9a and b). When patches

Table 1. Correlation matrices of landscape metrics applied to rectangular-patch landscapes under three types of disturbance growth, with all $r > |0.80|$ italicized.

Landscapes with enlarging patches (n = 50)

	P_j	Edge dens.	Contag.	Near. neigh. dist.	Prox. index	P-A fractal dim.	Mass fractal dim.
P_j	1.00	0.28	–0.13	–0.74	0.71	0.64	*–0.91*
Edge dens.		1.00	*–0.98*	–0.61	0.32	*0.90*	0.10
Contag.			1.00	0.55	–0.17	*–0.82*	–0.25
Near. neigh. dist.				1.00	–0.36	–0.79	0.58
Prox. index					1.00	0.54	–0.51
P-A fractal dim.						1.00	–0.30
Mass fractal dim.							1.00

Landscapes with abutting patches (n = 50)

	P_j	Edge dens.	Contag.	Near. neigh. dist.	Prox. index	P-A fractal dim.	Mass fractal dim.
P_j	1.00	0.47	–0.19	–0.77	0.42	0.65	*–0.92*
Edge dens.		1.00	*–0.93*	–0.62	0.61	*0.95*	–0.13
Contag.			1.00	0.53	–0.45	*–0.85*	–0.14
Near. neigh. dist.				1.00	–0.21	–0.78	0.64
Prox. index					1.00	0.55	–0.22
P-A fractal dim.						1.00	–0.37
Mass fractal dim.							1.00

Landscapes with buffered patches (n = 35)

	P_j	Edge dens.	Contag.	Near. neigh. dist.	Prox. index	P-A fractal dim.	Mass fractal dim.
P_j	1.00	*0.99*	*–0.99*	*–0.83*	*0.99*	0.53	*–0.88*
Edge dens.		1.00	*–0.97*	–0.78	*0.99*	0.49	*–0.83*
Contag.			1.00	*0.89*	*–0.99*	–0.61	*0.93*
Near. neigh. dist.				1.00	*–0.84*	*–0.82*	*0.91*
Prox. index					1.00	0.52	*–0.89*
P-A fractal dim.						1.00	–0.66
Mass fractal dim.							1.00

were buffered, however, patch size had less effect on fractal dimension values (Fig. 9c). The slopes derived from small, irregular patch landscapes and clearcut landscapes were statistically different (Table 6), but the values derived from each landscape series overlapped substantially (Fig. 9c). Thus, there was a statistical but not practical difference in values due to patch size.

Mass fractal dimension was fairly insensitive to differences in patch size, yielding similar-appearing response curves for both small-patch and large-patch landscapes (Fig. 10). Although we found a significant difference in slope for mass fractal dimension over increasing disturbance between clearcut landscapes and the two small-patch landscapes ($p < 0.001$, Tables 4, 5, and 6), the significance was due to low variance

Table 2. Correlation matrices of landscape metrics applied to landscapes with small, irregular-shaped patches under three types of disturbance growth, with all $r > |0.80|$ italicized.

Landscapes with enlarging patches (n = 50)

	P_j	Edge dens.	Contag.	Near. neigh. dist.	Prox. index	P-A fractal dim.	Mass fractal dim.
P_j	1.00	0.25	–0.12	–0.71	0.75	0.42	*–0.91*
Edge dens.		1.00	*–0.99*	–0.61	0.31	*0.94*	0.14
Contag.			1.00	0.57	–0.18	*–0.92*	–0.26
Near. neigh. dist.				1.00	–0.40	*–0.81*	0.53
Prox. index					1.00	0.33	–0.55
P-A fractal dim.						1.00	–0.08
Mass fractal dim.							1.00

Landscapes with abutting patches (n = 50)

	P_j	Edge dens.	Contag.	Near. neigh. dist.	Prox. index	P-A fractal dim.	Mass fractal dim.
P_j	1.00	0.42	–0.16	–0.76	0.43	0.61	*–0.89*
Edge dens.		1.00	*–0.94*	–0.55	0.73	*0.91*	–0.03
Contag.			1.00	0.48	–0.55	*–0.85*	–0.19
Near. neigh. dist.				1.00	–0.23	*–0.82*	0.64
Prox. index					1.00	0.55	–0.11
P-A fractal dim.						1.00	–0.30
Mass fractal dim.							1.00

Landscapes with buffered patches (n = 30)

	P_j	Edge dens.	Contag.	Near. neigh. dist.	Prox. index	P-A fractal dim.	Mass fractal dim.
P_j	1.00	*0.99*	*–0.99*	*–0.82*	*0.99*	0.68	*–0.95*
Edge dens.		1.00	*–0.98*	–0.79	*0.99*	0.65	*–0.93*
Contag.			1.00	*0.88*	*–0.99*	–0.75	*0.97*
Near. neigh. dist.				1.00	*–0.85*	*–0.86*	*0.90*
Prox. index					1.00	0.72	*–0.95*
P-A fractal dim.						1.00	–0.78
Mass fractal dim.							1.00

in fractal values among landscapes, and the actual difference in fractal values was extremely small.

Effects of patch shape

We examined differences between rectangular patch and small-irregular patch landscapes to evaluate the effects of patch shape on the fragmentation measures, since these two patch types differed only in shape. We found significant differences in response curves between rectangular patch and small-irregular patch landscapes for edge density, contagion, and perimeter-area fractal dimension under all modes of disturbance growth (Tables 4, 5, and 6). We found significant differences for mass fractal dimension only when disturbance increased through enlarging patches (Table 4).

Table 3. Correlation matrices for landscape metrics applied to landscapes with clearcut patches, under three types of disturbance growth, with all $r > |0.80|$ italicized.

Landscapes with enlarging patches (n = 50)

	P_j	Edge dens.	Contag.	Near. neigh. dist.	Prox. index	P-A fractal dim.	Mass fractal dim.
P_j	1.00	0.40	–0.12	–0.71	0.41	0.35	*–0.91*
Edge dens.		1.00	*–0.94*	–0.64	0.42	*0.85*	–0.04
Contag.			1.00	0.54	–0.27	*–0.85*	–0.23
Near. neigh. dist.				1.00	–0.27	–0.79	0.53
Prox. index					1.00	0.29	–0.25
P-A fractal dim.						1.00	–0.07
Mass fractal dim.							1.00

Landscapes with abutting patches (n = 40)

	P_j	Edge dens.	Contag.	Near. neigh. dist.	Prox. index	P-A fractal dim.	Mass fractal dim.
P_j	1.00	*0.99*	*–0.93*	–0.74	0.75	*0.92*	*–0.99*
Edge dens.		1.00	*–0.91*	–0.70	0.77	*0.91*	*–0.99*
Contag.			1.00	*0.87*	–0.50	*–0.92*	*0.92*
Near. neigh. dist.				1.00	–0.35	*–0.80*	0.73
Prox. index					1.00	0.67	–0.75
P-A fractal dim.						1.00	*–0.92*
Mass fractal dim.							1.00

Landscapes with buffered patches (n = 40)

	P_j	Edge dens.	Contag.	Near. neigh. dist.	Prox. index	P-A fractal dim.	Mass fractal dim.
P_j	1.00	*0.99*	*–0.99*	–0.77	*0.93*	0.73	*–0.98*
Edge dens.		1.00	*–0.97*	–0.73	*0.93*	0.67	*–0.98*
Contag.			1.00	*0.84*	*–0.92*	*–0.80*	*0.96*
Near. neigh. dist.				1.00	–0.78	*–0.85*	0.72
Prox. index					1.00	0.68	*–0.91*
P-A fractal dim.						1.00	–0.70
Mass fractal dim.							1.00

We found no evidence that patch shape influenced the nearest neighbor distance measure or mean proximity index. Neither the slopes or intercepts of rectangular or irregular patches were statistically different (Tables 4, 5, and 6), and the response curves appeared qualitatively similar (Figs. 7 and 8).

Effects from type of disturbance growth

We identified differences due to type of disturbance growth for most of the fragmentation measures tested, either in the magnitude of the observed values or in the general shapes of the response curves. Enlarging patches had less edge density than abutting or buffered patches (Fig. 5). Type of disturbance growth also influenced the point of maximum edge density, occurring

Table 4. Comparison of fragmentation measures when the enlarging patch rule was used to construct the landscapes. Comparisons are between rectangular-patch landscapes (R, *n* = 50), small-irregular-patch landscapes (S, *n* = 50), and clearcut-patch landscapes (C, *n* = 50).

Variables	Model[a]	R^2	d.f.	F	p > F	T-test	Comparison	T	p > T
Edge density	$Y = T + P + P^2$	0.99	8,	1701.9	0.001	R vs S	Patch shape	–6.35	0.001
	$+ TP + TP^2$		141			S vs C	Patch size	–29.93	0.001
						R vs C	Size and shape	–23.59	0.001
Contagion	$Y=T + P + P^2$	0.99	8m	4012.2	0.001	R vs S	Patch shape	2.56	0.012
	$+ TP + TP^2$		141			S vs C	Patch size	16.38	0.001
						R vs C	Size and shape	13.82	0.001
Near-neigh. dist.	ln(Y) = T + ln(P)	0.92[b]	5,	342.3	0.001	R vs S	Patch shape	–0.23	0.814
	+ T ln(P)		144			S vs C	Patch size	10.91	0.001
						R vs C	Size and shape	10.07	0.001
Perim-area fractal	$Y = T + P + P^2$	0.93	6,	302.3	0.001	R vs S	Patch shape	–5.53	0.001
	+ TP		143			S vs C	Patch size	24.07	0.001
						R vs C	Size and shape	5.79	0.001
Mass fractal	$Y = T + P + P^2$	0.98	6,	879.4	0.001	R vs S	Patch shape	1.01	0.317
	+ TP		128			S vs C	Patch size	4.75	0.001
						R vs C	Size and shape	4.17	0.001

[a]Y = the fragmentation measure, T = patch type (*n* = 50 for each type) and P = the proportion of the map disturbed by patch placement.
[b]Derived from log scale.

Table 5. Comparison of fragmentation measures when the abutting patch placement rule was used to construct the landscapes. Comparisons are between rectangular-patch landscapes (R, *n* = 50), small, irregular-patch landscapes (S, *n* = 50), and clearcut-patch landscapes (C, *n* = 40).

Variables	Model[a]	R^2	d.f.	F	p > F	T-test	Comparison	T	p > T
Edge density	$Y = T + P + P^2$	0.96	8,	544.4	0.001	R vs S	Patch shape	–4.05	0.001
	$+ TP + TP^2$		161			S vs C	Patch size	–18.52	0.001
						R vs C	Size and shape	–15.64	0.001
Contagion	$Y = T + P + P^2$	0.99	8,	4996.5	0.001	R vs S	Patch shape	2.94	0.004
	$+ TP + TP^2$		161			S vs C	Patch size	22.35	0.001
						R vs C	Size and shape	20.27	0.001
Near-neigh. dist.	ln(Y) = T + ln(P)	0.95[b]	5,	596.2	0.001	R vs S	Patch shape	–0.62	0.539
	+ T ln(P)		164			S vs C	Patch size	13.59	0.001
						R vs C	Size and shape	12.74	0.001
Perim-area fractal	$Y = T + P + P^2$	0.93	8,	282.5	0.001	R vs S	Patch shape	–4.91	0.001
	$+ TP + TP^2$		161			S vs C	Patch size	–4.68	0.001
						R vs C	Size and shape	–5.57	0.001
Mass fractal	Y = T + P + TP	0.98	5,	1725.3	0.001	R vs S	Patch shape	6.79	0.001
			154			S vs C	Patch size	15.70	0.001
						R vs C	Size and shape	9.01	0.001

[a]Y = the fragmentation variable, T = patch type, and P = the proportion of the landscape disturbed by patch placement.
[b]Derived from log scale.

near $P_j = 0.60$ for enlarging patches, around $P_j = 0.65$ for abutting patch landscapes, and at the maximum P_j for buffered patch landscapes, between 0.30–0.40.

For contagion, type of disturbance growth had the most pronounced effect at mid-ranges of disturbance. For example, at $P_j = 0.35$, contagion of rectangular-patch landscapes was approximately 12% higher when patches enlarged than when patches were buffered (Fig. 6).

Table 6. Comparison of fragmentation measures when the buffered patch placement rule was used to construct the landscapes. Comparisons are between rectangular-patch landscapes (R, n = 35), small-irregular-patch landscapes (S, n = 35), and clearcut-patch landscapes (C, n = 40).

Variables	Model[a]	R^2	d.f.	F	$p > F$	T-test	Comparison	T	$p > T$
Edge density	$Y = T + P + P^2$	0.99	8,	4139.8	0.001	R vs S	Patch shape	–7.16	0.001
	$+ TP + TP^2$		96			S vs C	Patch size	3.94	0.001
						R vs C	Size and shape	6.87	0.001
Contagion	$Y = T + P_i + P^2$	0.99	8,	12026.4	0.001	R vs S	Patch shape	2.91	0.005
						S vs C	Patch size	7.42	0.001
	$+ TP + TP^2$		96			R vs C	Size and shape	5.78	0.001
Near-neigh. dist.	$\ln(Y) = T + \ln(P)$	0.95[b]	5,	389.7	0.001	R vs S	Patch shape	–1.25	0.215
	$+ T \ln(P)$		99			S vs C	Patch size	6.69	0.001
						R vs C	Size and shape	8.36	0.001
Perim-area fractal	$Y = T + P + P^2$	0.87	8,	81.6	0.001	R vs S	Patch shape	13.03	0.001
	$+ TP + TP^2$		96			S vs C	Size and shape	3.98	0.001
Mass fractal	$Y = T + P_i + TP$	0.96	3,	461.3	0.001	R vs S	Patch shape	13.3	*
			61			S vs C	Patch size	*	*
						R vs C	Size and shape	*	*

[a] Y = the fragmentation variable, T = patch type, and P = the proportion of the landscape disturbed by patch placement.
[b] Derived from log scale.
* Qualitatively different; no statistical test performed; see text

Mean nearest neighbor distance and mean proximity index appeared insensitive to type of disturbance growth. All landscape series yielded similar response curves and similar ranges of values (Figs. 7 and 8).

For perimeter-area fractal dimension, type of disturbance growth affected both the magnitude of values and shape of response curves, especially for landscapes consisting of rectangular patches (Fig. 9). Enlarging and abutting patch rules allowed rectangles to coalesce into irregular shapes, resulting in higher perimeter-area fractal values than under the buffered patch rule, which maintained the original, rectangular shapes. The abutting patch rule yielded higher fractal dimension values than either the overlapping or buffered patch rules. Response curves were flattest for buffered patch landscapes.

Mass fractal dimension was minimally affected by type of disturbance growth. However, enlarging patches yielded the greatest range of observed values, and was the only growth pattern that resulted in fractal dimension values < 1 (Fig. 10). This appeared to be an artifact of the small extent of our 101×101 pixel maps. Using maps with either 256^2 or 512^2 pixels, the lowest values derived were 1.12 and 1.19 respectively, similar to those derived under the other growth models.

Sensitivity to the spatial distribution of patches

To test for sensitivity to the spatial distribution of patches, we compared the values of each landscape measure when applied to landscapes having the same level of disturbance, but with patches either dispersed or aggregated (Fig. 4). None of the measures were able to distinguish spatial distribution of patches in a meaningful way (Fig. 11). Landscapes with aggregated patches had slightly higher edge density values than landscapes with dispersed patches, but the response curves were nearly the same (Fig. 11a). Contagion values were also similar for both aggregated and dispersed patches (Fig. 11b). The slight differences between response curves for both of these measures was due to patch size selected by the LSF algorithm: dispersed-patch landscapes used smaller patches to fill the remaining space when disturbance was high, resulting in slightly higher edge density and slightly lower contagion values.

Mean nearest neighbor distance values declined with increasing disturbance when patches were dispersed, but were uniformly low when landscapes were aggregated (Fig. 11c). Landscapes with tightly aggregated patches produced the same values as landscapes with high disturbance and dispersed patches because the distance between aggregated patches was the same as that of a highly disturbed landscape. The nearest

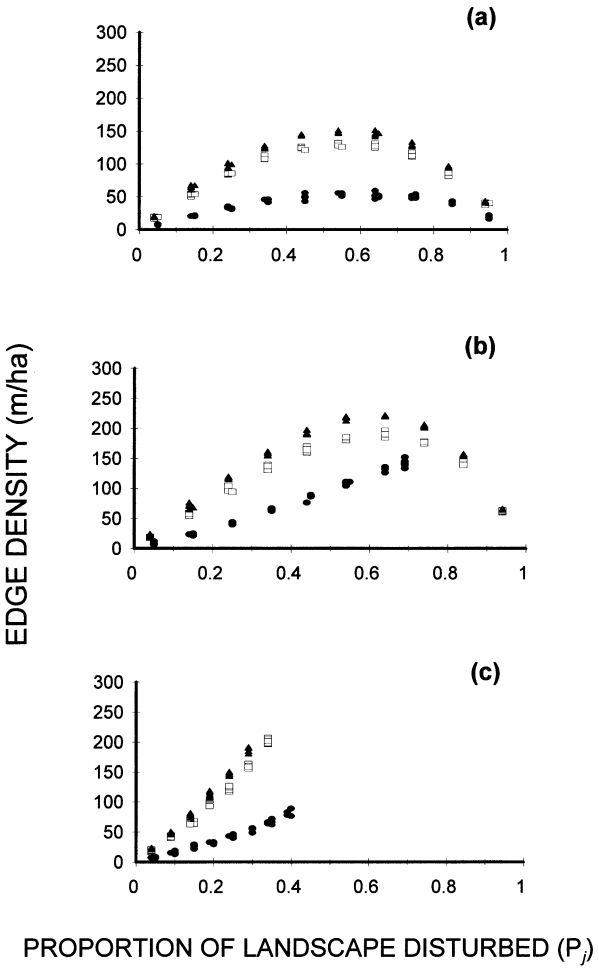

Figure 5. Values of edge density derived from landscapes with different modes of disturbance: a) enlarging patches; b) abutting patches; and c) buffered patches. Multiple symbols at each level of disturbance represent 5 simulations per patch type. □ = rectangular patch landscapes ▲ = small-irregular patch landscapes ● = clearcut landscapes.

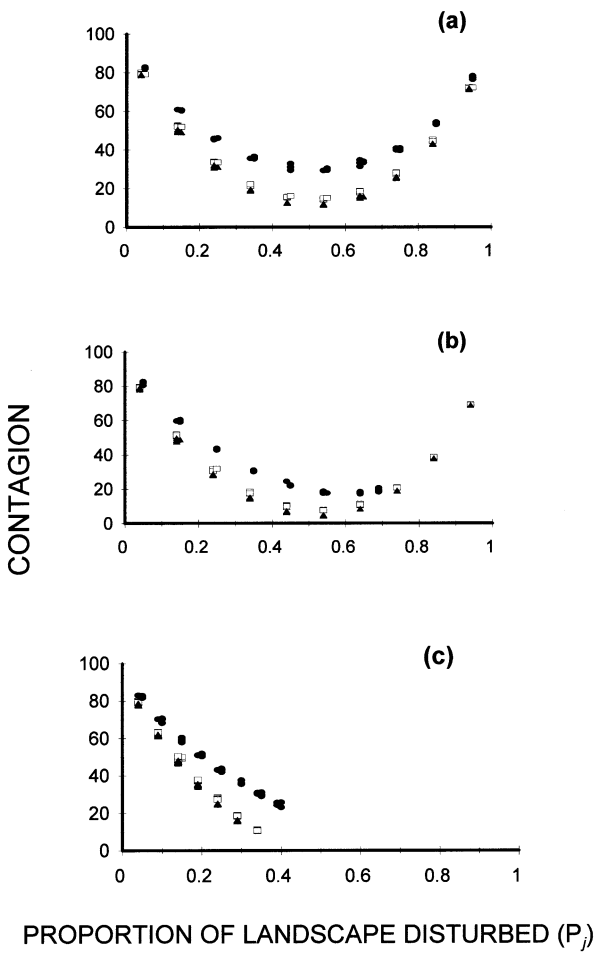

Figure 6. Values of contagion derived from landscapes with different modes of disturbance: a) enlarging patches; b) abutting patches; and c) buffered patches. Multiple symbols at each level of disturbance represent 5 simulations per patch type. □ = rectangular patch landscapes ▲ = small-irregular patch landscapes ● = clearcut landscapes.

neighbor distance measure does not include the distance between a patch and the edge of the landscape window, and thus cannot differentiate between a landscape that contains three patches each 30 m apart in one corner of the landscape window, and a landscape that is filled with patches that on average are 30 m apart.

Mean proximity index appeared more sensitive to patch distribution, in that landscapes with aggregated patches had consistently higher values than landscapes with dispersed patches (Fig. 11d). However, aggregated patch landscapes at P_j = 0.10 had nearly the same mean proxmity index values as landscapes at P_j = 0.40, so the usefulness in differentiating landscape pattern was still limited. Again, this was because the measure does not place patch location in the context of the landscape window.

Neither of the measures of fractal dimension provided unique values for landscapes with aggregated versus dispersed patches (Fig. 11e and f). Mass fractal dimension values were slightly lower for aggregated patch landscapes, but the response curves for both landscape patterns were the same.

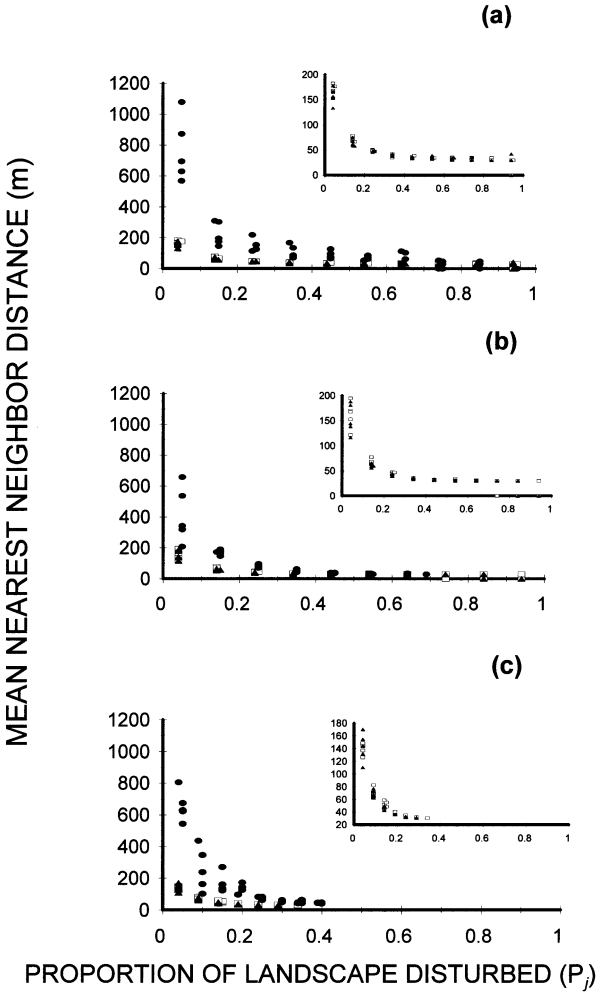

Figure 7. Values of mean nearest neighbor distance derived from landscapes with different modes of disturbance: a) enlarging patches; b) abutting patches; and c) buffered patches. Multiple symbols at each level of disturbance represent 5 simulations per patch type. □ = rectangular patch landscapes ▲ = small-irregular patch landscapes ● = clearcut landscapes. Inserts show similarity in the shapes of response functions when rectangular patch landscapes and small-irregular patch landscapes are graphed at a larger scale.

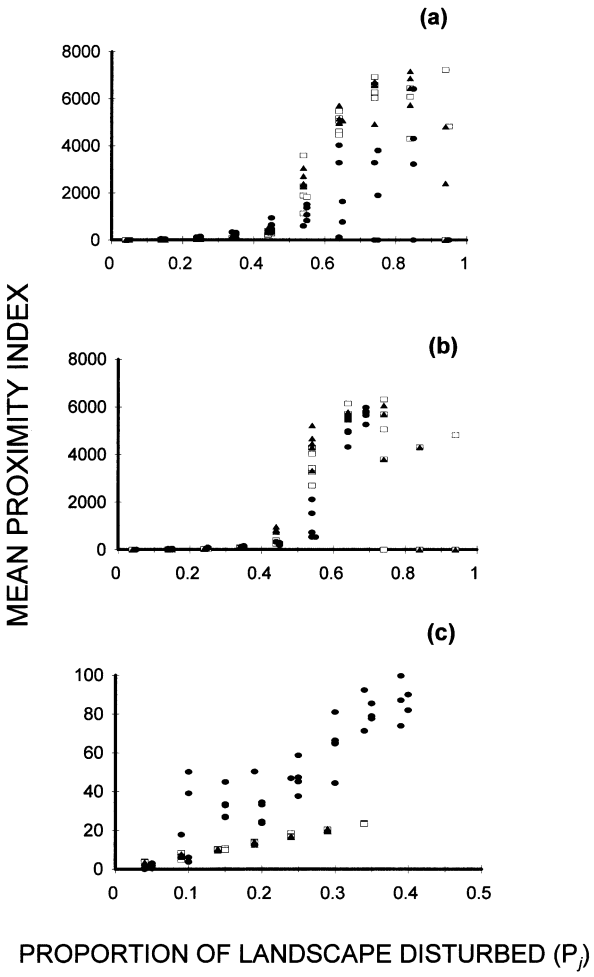

Figure 8. Values of mean proximity index derived from landscapes with different modes of disturbance: a) enlarging patches; b) abutting patches; and c) buffered patches. Buffered patch landscapes are graphed on a larger scale for visibility. Multiple symbols at each level of disturbance represent 5 simulations per patch type. □ = rectangular patch landscapes ▲ = small-irregular patch landscapes ● = clearcut landscapes.

Discussion

It is essential to know whether a particular measure provides a unique contribution to our understanding of landscape structure and habitat fragmentation, or simply repeats information provided by other measures and by the proportion of disturbance. Correlation is somewhat expected because all spatial metrics are based on a limited number of basic parameters: patch size, shape, perimeter-area ratio, and interpatch distance (Li et al. 1993).

Ritters et al. (1995) investigated 55 metrics, and found that these could be reduced to six general measures of landscape pattern and structure: average perimeter-area ratio, contagion, standardized patch shape, patch perimeter-area scaling, number of attribute classes, and large-patch density-area scaling. Their analysis differed from ours in that the metrics were applied to actual landscapes rather than simulations, and therefore correlations were generally lower, with only 11 out of 325 Pearson's correlation coefficients having absolute values > 0.80 (Ritters et al. 1995). Correlations between all combinations of edge

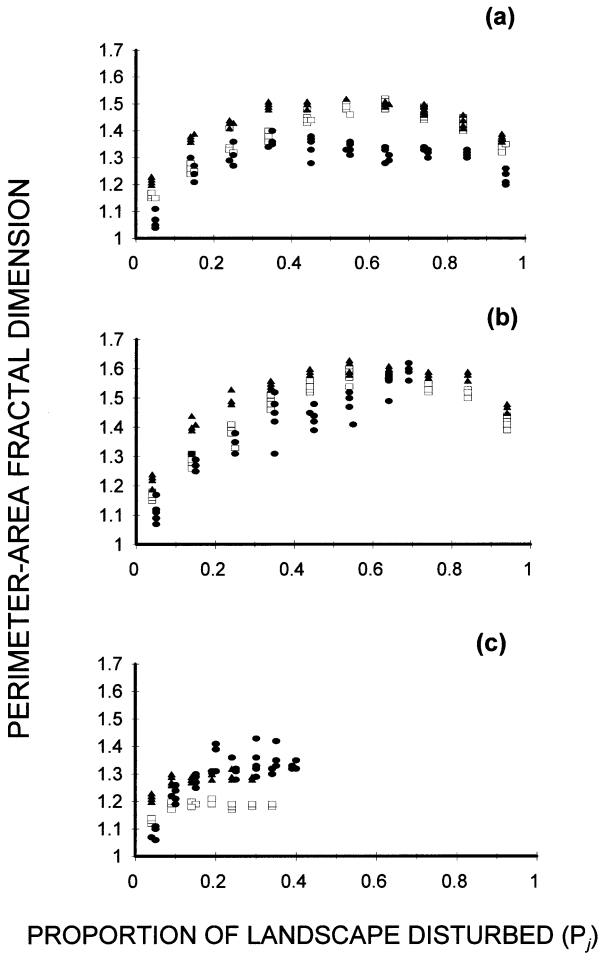

Figure 9. Values of perimeter-area fractal dimension derived from landscapes with different modes of disturbance: a) enlarging patches; b) abutting patches; and c) buffered patches. Multiple symbols at each level of disturbance represent 5 simulations per patch type. □ = rectangular patch landscapes ▲ = small-irregular patch landscapes ● = clearcut landscapes.

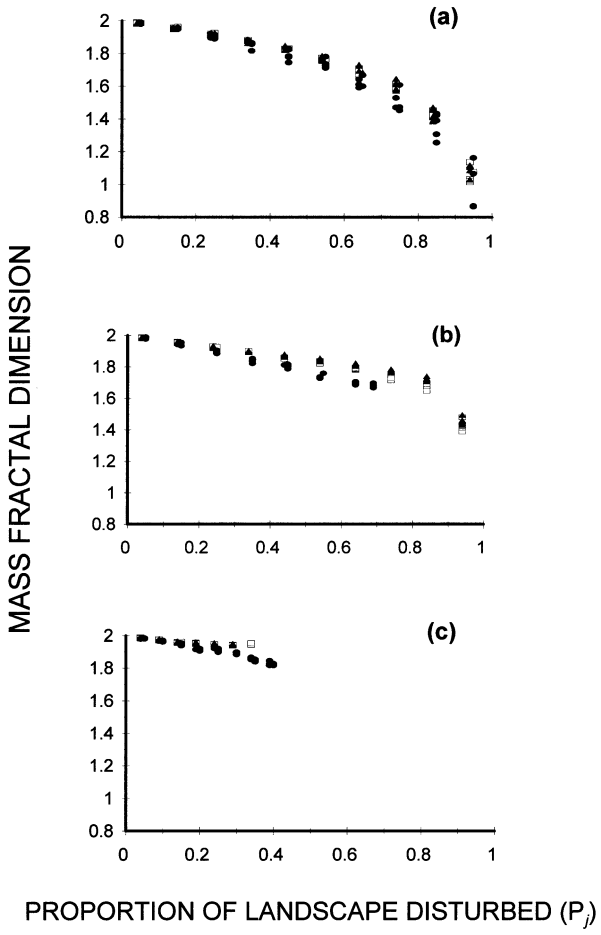

Figure 10. Values of mass fractal dimension derived from landscapes with different modes of disturbance: a) enlarging patches; b) abutting patches; and c) buffered patches. Multiple symbols at each level of disturbance represent 5 simulations per patch type. □ = rectangular patch landscapes ▲ = small-irregular patch landscapes ● = clearcut landscapes.

density, contagion, perimeter-area fractal dimension, and mass fractal dimension, which they referred to as PORO, SHCO, OEFC, and PMAS respectively, were significant at $p = 0.01$, although absolute values of Pearson's correlation coefficients were between 0.24–0.46 (Ritters et al. 1995), whereas ours were generally > 0.90 for the same measures (Tables 1, 2, and 3).

Our analysis included measures of interpatch distance that were not evaluated by Ritters et al. (1995). We found mean nearest neighbor distance and mean proximity distance to have comparatively low correlations with other metrics, and suggest that some measure of interpatch distance should be added to the minimal subset of landscape metrics proposed by Ritters et al.(1995).

Each of the metrics we examined had strengths and weaknesses in quantifiying one or more components of landscape structure. In the following section, we describe the potential usefulness of each measure while highlighting drawbacks and limitations.

Edge density

A primary outcome of habitat fragmentation is an increase in habitat edge, which is effectively quantified with edge density. This measure is entirely dependent on the ratio of patch area to patch edge, and landscapes

with small patches or irregular shapes will have higher edge density values than landscapes with large patches or simple shapes at the same proportion of disturbance.

It is intuitive that edge density will increase with increasing representation of a disturbance cover type. However, if disturbance patches can coalesce or grow in size, edge density will eventually decline at successive levels of disturbance, because of the increase in patch area-to-edge ratio. As a consequence, both low- and high-disturbance landscapes have similar edge values, making it difficult to observe correlations between edge density and ecological phenomena over increasing disturbance. Many ecological questions are addressed over a narrow range of fragmentation, and duplicate values at different levels of disturbance generally are not a problem. Over narrow ranges, edge density is linearly correlated with change in the amount of disturbance, with the slope of the relationship determined by patch size and irregularity of patch edge.

Edge density is an effective tool for evaluating the effects of patch shape and area on the abundance of habitat edge. Wallin et al. (1994) used edge density to evaluate differences in dispersed versus aggregated timber harvest patterns, and found higher values with dispersed cutting. Since edge density is not sensitive to spatial pattern, the differences reported were due to differences in patch size used to create dispersed and aggregated harvest units rather than differences in harvest pattern.

Contagion

Contagion indices are designed to quantify the degree of aggregation found within cover types on a landscape (O'Neill et al. 1988, Li and Reynolds 1993). Contagion has been interpreted further to measure the interspersion of different patch types, as well as aggregation within a patch type (McGarigal and Marks 1995). We found, however, that contagion is insensitive to landscape patterns in which patches are either widely dispersed or tightly clustered (Fig. 11b). Although a clustered disturbance produces greater aggregation of original habitat (Fig. 4), there is no increase in contagion value compared to dispersed-patch landscapes.

Contagion and edge density have a strong, negative correlation because both are based on the occurrence of edge pixels in a landscape. Rogers (1993) highlights the association between contagion and edge by defining contagion as the frequency of occurrence of all possible edge types within a landscape. Both measures reflect the degree by which any given cover type is aggregated by means of patch size and shape. High aggregation occurs when patch area is large relative to patch edge length, resulting in simultaneously low values of edge and high values of contagion. Aggregation is not a measurement of the clustering of several patches into one area of a landscape. Thus, contagion reflects the area:edge ratio of patches rather than the spatial arrangement of patches, and is inversely related to edge density.

Since edge density and contagion provide highly correlated information, use of both measures to quantify landscape pattern is somewhat redundant. Choice of measure depends on the nature of the investigation. For example, the relationship between contagion and percolation theory (Gardner and O'Neill 1991) may seem intuitively easier to understand than edge and percolation theory, whereas habitat ecotones are best quantified by edge density (McGarigal and McComb 1995).

Mean nearest neighbor distance

Mean nearest neighbor distance provides information on spacing between patches in a cluster, a distance that grows exponentially shorter with increasing disturbance, regardless of the patch type or mode of disturbance growth (see also Gustafson and Parker 1992, Andrén 1994). When disturbance exceeds 0.20, this measure provides a range of values so narrow that discrimination among landscapes is difficult. However, the high variance in values when disturbance is < 0.20 suggests that this metric may be useful in differentiating inter-patch distances when fragmentation is low. Likewise, it could be used to assess distances between remnant patches of original habitat when disturbance is high.

The mean nearest neighbor distance measure is limited in applicability because it requires landscapes of similar extent and known grain for comparative studies. As with the other metrics examined, it also does not adequately describe the spatial distribution of patches. A landscape with all patches clumped can produce the same mean value as a landscape with widely-dispersed pairs of patches (Rogers 1993). This difficulty can be somewhat overcome by reporting the standard deviation around the mean, which can serve as a measure of patch dispersion (McGarigal and Marks 1995). However, the greatest shortcoming with this measure is the inability to include the entire

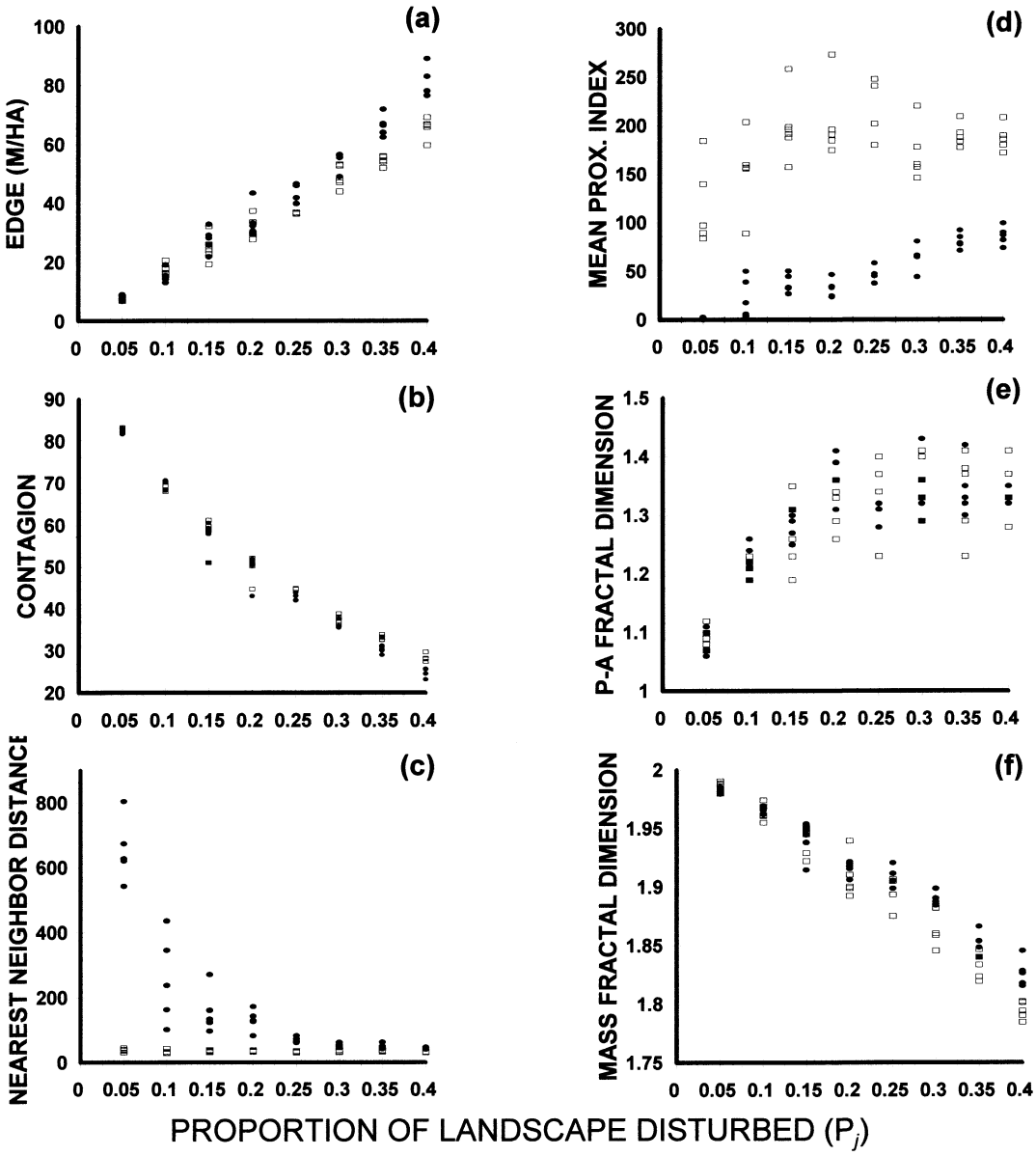

Figure 11. Response functions for six landscape metrics on simulated landscapes with either aggregated or dispersed patches. □ = aggregated patches; • = dispersed patches

extent of a landscape in the calculations. The measure only applies to distances between patches in a cluster, ignoring the potentially vast distance between the edge of the cluster and the edge of the map (Fig. 4).

Mean proximity index

The proximity index is an effective measure of patch isolation for either remnant or disturbances patches. A notable property of this index is the radical change in values associated with percolation of the disturbance across the landscape (Gustafson and Parker 1992). The proximity index is influenced by percolation and demonstrates a sigmoid response curve with increas-

ing P_j (Fig. 8) that resembles the percolation probability curve for landscapes with contagion (Gardner and O'Neill 1991). On infinitely large maps containing random pixels of two cover types, percolation of a cover type through the four adjacent pixels occurs when that type occupies 0.5928 of the map space (Stauffer 1985). Contagion broadens the critical probability to occur within a range of approximately 0.50–0.65 (Gardner and O'Neill 1991). In our simulations, the dramatic increase in values of the mean proximity index indicates the approximate point of percolation for each artificial landscape. When disturbance growth is with buffered patches, the buffers restrict the disturbance from percolating, and the proximity index is truncated below the inflection point associated with percolation, creating a linear rather than sigmoid response curve (Fig. 8c).

Patch size affects the proximity index, since area is used in calculating this measure. Slight differences in the spatial distribution of patches can substantially alter patch size. Shifting a patch location by one pixel can result in the coalescence of two small patches into one larger patch, substantially increasing the average area of all patches within the search radius. However, slight changes in the distance between patches has more effect than patch size. Shifting a patch so that the distance between it and a neighboring patch is a full pixel away rather than abutting diagonally will result in a substantial increase in the proximity index (Gustafson and Parker 1992).

Use of the proximity index is best for disturbance levels below the critical probability for percolation. Above this, the wide range of observed values caused by slight differences in spatial arrangement of patches may be difficult to interpret ecologically. The proximity index can be applied where patches of interest occur in low densities and under different degrees of isolation, such as in gap analysis of species distribution and the study of spatial patterns of metapopulations. Spetich et al. (1997) used the proximity index to quantify the relative isolation of old-growth forest patches in Indiana. The proximity index would be an excellent tool in studies similar to that of Dunn et al. (1991). They compared isolated versus proximal woodlots in Wisconsin to examine the role of woodlot size and spatial distribution in the future dispersal of tree species.

Perimeter-area fractal dimension

The perimeter-area fractal dimension used in our simulations is one of several measures of fractal dimension used in the analysis of geographical data (Burrough 1986; Olsen et al. 1993). It is applicable when the ecological question is related to the irregularity of patch edges and the effect of this irregularity on landscape pattern, and has an advantage over edge density and other edge measures in that values derived are theoretically scale invariant. However, scale invariance does not hold for landscapes that exhibit changes in pattern (aggregation) with changes in scale (Burrough 1981; Krummel et al. 1987; Turner et al. 1989; Milne 1992).

This measure is essentially a patch-level statistic and will not differentiate between landscapes if all patches exhibit similar irregularity. In our comparison of landscapes with buffered patches, the perimeter-area fractal dimension response curve was nearly flat across the range of increasing disturbance, because the average irregularity of individual patches did not change with the placement of additional patches (Fig. 9). An example of this limitation is found in Ripple et al. (1991), where a comparison of two landscapes with buffered patches yielded perimeter-area fractal dimension values of 1.26 and 1.28, although disturbance increased from 8.5% to 23%.

By averaging perimeter-area fractal dimension for all patches in a landscape, the prime utility of this measure is lost, which is information on individual patch shape. The landcape average is a mid-range value between one and two that provides no information on landscape pattern and smooths the information pertaining to individual patch shapes. The range of possible values is further constrained by mapping techniques, because the fractal nature of patch edge is constrained by the resolution of the map and the tendency to simplify borders when patches are delineated.

Although perimeter-area fractal dimension has limited ability to quantify landscape pattern or fragmentation, it has greater applicability in our understanding of scaling relationships between landforms and ecological processes. Milne (1994) used this measure to demonstrate the scaling relationship between coastline length of Admiralty Island, Alaska, and spacing of eagle nests along the coast, using data from Robards and Hodges (1976).

Mass fractal dimension

Mass fractal dimension has been used to quantify the configuration of landscape matrices created by patches. The shape of the mass fractal dimension response curve with increasing disturbance reflects the phenomenon of percolation, and most of the change in fractal dimension values occurs after percolation of disturbance, as shown by the steepened response curve after $P_j = 0.55$, especially in landscapes with enlarging patches (Fig. 10).

Mass fractal dimension values are scarcely altered by size and shape of patches, as evidenced by similarity in response curves for all patch configurations (Fig. 10). We tested this conclusion by measuring mass fractal dimension on a series of maps constructed from randomly-placed pixels in which we varied the proportional representation of two pixel classifications at 0.10 intervals in the same manner as with our other simulations. We obtained a response curve similar to that of landscapes with overlapping patches, with fractal dimension values decreasing from 1.99 to 1.25. Thus, mass fractal dimension did not discriminate between landscapes containing random pixels and landscapes containing fairly large patches at the same level of disturbance.

Mass fractal dimension is highly correlated with increase in disturbance, resulting in correlation coefficients between –0.89 and –0.98 for the patch configurations and growth patterns we simulated (Tables 1, 2, and 3). This finding, coupled with the inability to distinguish patterns of clumped versus dispersed patches, suggest that mass fractal dimension may have little utility for discriminating landscapes with differing sizes and shapes of patches. This is partly because the inherent fractal nature of landscapes was removed by smoothing and simplfying the perimeters of patches used in our simulations. However, similar mapping processes are used on many classified GIS images, and thus, mass fractal dimension may have limited applicability on map images where smoothing and renormalization functions have been applied. As with perimeter-area fractal dimension, the strength of this measure may be in the investigation of scaling relationships between organisms and their environment. Milne et al. (1992) used fractal geometry to characterize resource abundance at various scales, and investigated allometric relationships between three sizes of herbivores and fractally-distributed resources. Ritchie and Moroge (in prep.) demonstrated that organisms viewing the environment on a large scale are more sensitive to habitat fragmentation than small-scale organisms, when the scaling relationship is considered from a fractal rather than Euclidean perspective.

Conclusion

Landscape metrics are developed to measure varying aspects of landscape structure, yet they are interrelated by their dependency on the same underlying measures of patch area, edge length, and inter-patch distance. In spite of the mathematical kinship, most measures we examined provide unique information about landscapes not contained in other metrics. The notable exceptions are contagion and edge density, which have near-perfect, inverse correspondence, because both measures are based on the proportion of edge pixels in a landscape. Perimeter-area fractal dimension also is related to contagion and edge density, although less strongly, because of dependency on patch area and edge length in calculations. The correlation among all measures is greatest over disturbance levels < 0.40, because all measures except mean nearest neighbor distance exhibit the greatest linearity over this range.

The measures we examined were relatively insensitive to variations in the spatial arrangement of patches on a landscape. Mean nearest neighbor distance and mean proximity index both quantify distances between patches in a cluster, but neither are designed to place the cluster in the context of the landscape window. Edge density, contagion, and perimeter-area fractal dimension are all metrics of landscape pattern caused by size and shape of patches and their proportional representation on a landscape, but none can differentiate the spatial relationship among patches.

Although the equations for these measures include no factors for measuring spatial arrangement, many ecologists assume that certain landscape metrics, particularly contagion, mean nearest neighbor distance, mean proximity index, and mass fractal dimension, are able to detect these differences. This belief is supported by several published papers where authors have used phrases that imply sensitivity to spatial distribution. For example, the FRAGSTATS manual states, “Contagion measures both patch type interspersion (i.e., the intermixing of units of different patch types) as well as patch dispersion (i.e., the spatial distribution of a patch type)” (McGarigal and Marks 1995, p. 57). In a comparative study, Wallin et al. (1994) observed differences in edge density between “dispersed” and “aggregated” timber harvest patterns,

terms that emphasize the spatial distribution of the harvest blocks. Their results are valid, but should be attributed to patch size (dispersed patches were substantially smaller than aggregated patches) rather than patch dispersion. Likewise, Li et al. (1993) tested for differences in "random patch" harvest models versus "partial aggregation", and other spatial distributions. Their discussion implied sensitivity to spatial arrangement that should have been attributed to patch size and shape. Ecologists are interested in spatial distribution of patches, because many processes, including climatic factors, seed dispersal, and animal behavior are potentially influenced by this component of landscapes. At present, however, we are not aware of a landscape metric that quantifies spatial arrangement. It may be possible to alter mean proximity index or nearest neighbor distance to provide information on the distance from each patch to a point or points at the edge of the specified landscape window. In the absence of such a measure, ecologists can increase their understanding of landscape processes by applying several metrics to any given investigation (Rogers 1993; McGarigal and McComb 1995; Ritters et al. 1995).

Ecologists using the measures we have discussed can benefit by understanding the attainable values of each metric, and how these values are altered within landscapes containing different sizes and shapes of patches, and different modes of disturbance. We have provided graphical representations of the attainable values derived from our simulations to assist ecologists in interpreting the values achieved for actual landscapes. Source code and documentation for the LSF program are available at http://www.arc.unm.edu/lsf.

Acknowledgments

We appreciate use of the FRAGSTATS spatial pattern analysis program developed by K. McGarigal and B. Marks at Oregon State University, and we thank B. Milne and T. Keitt at the University of New Mexico for use of their software for calculating the mass fractal dimension. Thanks to D. Turner of the Intermountain Research Station, Logan, Utah, and S. Durham at Utah State University for statistical consultation. We appreciate comments and suggestions on this manuscript from B. Milne, J. Long, M. Ritchie, and M. Conover. Use of the supercomputer at the Albuquerque Resource Center was sponsored in part by the Phillips Laboratory, Air Force Materiel Command, USAF, under cooperative agreement number F29601–93–2–0001. The views and conclusions contained in this document are those of the authors and should not be interpreted as necessarily representing the official policies or endorsements of Phillips Laboratory or the U.S. government. We acknowledge use of the KHOROS® software development environment. KHOROS® is a registered trademark of Khoral Research, Inc.

References

Andrén, H. Effects of habitat fragmentation on birds and mammals in landscapes with different proportions of suitable habitat: a review. Oikos 71: 355–366.

Burrough, P.A. 1981. Fractal dimensions of landscapes and other environmental data. Nature 294: 240–242.

Burrough, P.A. 1986. Principles of geographic information systems for land resources assessment. Oxford University Press, New York.

Department of Agriculture. 1982. National Forest System land and resource management planning. 36 CFR Part 219. Fed. Reg. 47: 43051.

Dunn, C.P., D.M. Sharpe, G.R. Guntenspergen, F. Stearns and Z. Yang. 1991. Methods for analyzing temporal changes in landscape pattern. *In* Quantitative Methods in Landscape Ecology. pp. 173–198. Edited by M.G. Turner and R.H. Gardner. Springer-Verlag, New York.

Forman, R.T.T. and M. Godron. 1986. Landscape ecology. John Wiley and Sons, New York.

Gardner, R.H. and R.V. O'Neill. 1991. Pattern, process, and predictability: the use of neutral models for landscape analysis. *In* Quantitative Methods in Landscape Ecology. pp. 289–307. Edited by M.G. Turner and R.H. Gardner. Springer-Verlag, New York.

Grossman, T. and A. Aharony. 1987. Accessible external perimeters of percolation clusters. J. Phys. A: Math Gen. 20: L1193-L1201.

Gustafson, E.J. and G.R. Parker. 1992. Relationships between landcover proportion and indices of landscape spatial pattern. Landscape Ecol. 7: 101–110.

Kleinbaum, D.G., L.L. Kupper and K.E. Muller. 1988. Applied regression analysis and other multivariate methods. Second edition. PWS-Kent, Boston, Mass.

Krummel, J.R., R.H. Gardner, G. Sugihara, R.V. O'Neill and P.R. Coleman. 1987. Landscape patterns in a disturbed environment. Oikos 48: 321–324.

Li, H. and J.F. Reynolds. 1993. A new contagion index to quantify spatial patterns of landscapes. Landscape Ecol. 8: 155–162.

Li, H., J.F. Franklin, F.J. Swanson and T.A. Spies. 1993. Developing alternative forest cutting patterns: a simulation approach. Landscape Ecol. 8: 63–75.

Lovejoy, S. 1982. Area-perimeter relation for rain and cloud areas. Science 216: 185–187.

McGarigal, K. and B. Marks. 1995. FRAGSTATS: Spatial analysis program for quantifying landscape structure. USDA Forest Service Gen. Tech. Rep. PNW-GTR–351.

McGarigal, K. and W.C. McComb. 1995. Relationships between landscape structure and breeding birds in the Oregon coast range. Ecol. Mon. 65: 235–260.

Milne, B.T. 1991. Lessons from applying fractal models to landscape patterns. *In* Quantitative Methods in Landscape Ecology. pp. 199–235. Edited by M.G. Turner and R.H. Gardner. Springer-Verlag, New York.

Milne, B.T. 1992. Spatial aggregation and neutral models in fractal landscapes. Am. Nat. 139: 32–57.

Milne, B.T., M.G. Turner, J.A. Wiens and A.R. Johnson. 1992. Interactions between the fractal geometry of landscapes and allometric herbivory. Theor. Pop. Biol. 41: 337–353.

Milne, B.T. 1994. Pattern analysis for landscape evaluation and characterization. *In* Eastside Forest Ecosystem Health Assessment. Vol. II.: Ecosystem Management: Principles and Applications. pp 121–134. Edited by M.E. Jensen and P.S. Bourgeron. USDA Forest Service Gen. Tech. Rep. PNW-GTR–318.

Musick, H.B. and H.D. Grover. 1991. Image textural measures as indices of landscape pattern. *In* Quantitative Methods in Landscape Ecology. pp. 289–307. Edited by M.G. Turner and R.H. Gardner. Springer-Verlag, New York.

Olsen, E.R., R.D. Ramsey and D.S. Winn. 1993. A modified fractal dimension as a measure of landscape diversity. Photogrammetric Eng. and Remote Sensing 59: 1517–1520.

O'Neill, R.V., J.R. Krummel, R.H. Gardner, G. Sugihara, B. Jackson, D.L. DeAngelis, B.T. Milne, M.G. Turner, B. Zygmunt, S.W. Christensen, V.H. Dale and R.L. Graham. 1988. Indices of landscape pattern. Landscape Ecol. 1: 153–162.

Ripple, W.J., G.A. Bradshaw and T.A. Spies. 1991. Measuring forest landscape patterns in the Cascade Range of Oregon, USA. Biol. Cons. 57: 73–88.

Ritchie, M. and M.A. Moroge. Scale dependent effects of habitat fragmentation on population density. In prep.

Ritters, K.H., R.V. O'Neill, C.T. Hunsaker, J.D. Wickham, D.H. Yankee, S.P. Timmins, K.B. Jones and B.L. Jackson. 1995. A factor analysis of landscape pattern and structure metrics. Landscape Ecology 10: 23–39.

Robards, F.C. and J.I. Hodges. 1976. Observations from 2,760 bald eagle nests in southeast Alaska: progress report 1969–1976. USDI Fish and Wildlife Service, Eagle management study, Juneau, AK.

Rogers, C.A. 1993. Describing landscapes: indices of structure. M.S. Thesis, Simon Fraser University, Burnaby, B.C.

Spetich, M.A., G.R. Parker and R.J. Gustafson. 1997. Spatial and temporal relationships of old-growth and secondary forests in Indiana. Natural Areas Journal 17: 118–130.

Spies, T.A., W.J. Ripple and G.A. Bradshaw. 1994. Dynamics and pattern of a managed coniferous forest landscape in Oregon. Ecol. Appl. 4: 555–568.

Stauffer, D. 1985. Introduction to percolation theory. Taylor and Francis, London.

Turner, M.G. 1990. Spatial and temporal analysis of landscape patterns. Landscape Ecol. 4: 21–30.

Turner, M.G., R.V. O'Neill, R.H. Gardner and B.T. Milne. 1989. Effects of changing spatial scale on the analysis of landscape pattern. Landscape Ecol. 3: 153–162.

Voss, R.F. 1984. The fractal dimension of percolation cluster hulls. J. Phys. A: Math. Gen. 17: L373-L377.

Voss, R.F. 1988. Fractals in nature: from characterization to simulation. *In* The Science of Fractal Images. pp. 21–70. Edited by H.O. Peitgen and D. Saupe. Springer-Verlag, New York.

Wallin, D.O., F.J. Swanson and B. Marks. 1994. Landscape pattern response to changes in pattern generation rules: land-use legacies in forestry. Ecol. Appl. 4: 569–580.

Whitcomb, R.F., C.S. Robbins, J.F. Lynch, B.L. Whitcomb, M.K. Klimkiewicz and D. Bystrak. 1981. Effects of forest fragmentation on avifauna of the eastern deciduous forest. *In* Forest island dynamics in man-dominated landscapes. pp. 125–205. Edited by R.L. Burgess and D.M. Sharpe. Springer-Verlag, New York.